

Impact of Aggregate Size on the Behavior of Steel Fiber Reinforced Concrete Deep Beams without stirrups

Y. M. Abbas

Assistant Professor, Department of Civil Engineering
King Saud University, Riyadh 800-11421, Saudi Arabia
Email: yabbas@ksu.edu.sa

Abstract

In this paper, the influence of aggregate size on the mechanical behavior of steel fiber reinforced concrete (SFRC) deep beams is reported. Two full-scale SFRC deep beams were developed with conventional concrete and tested under four-point conditions at 2 mm/min loading rate. The first beam was prepared with normal concrete of maximum aggregate size of 10 mm (CA10), whereas, the second beam was developed by 20 mm and 10 mm mixed coarse aggregate (CA20-10). Because of the improved fiber distribution, the ductility of SFRC deep beams with CA10 was marginally higher and had notably higher load capacity with respect to CA20-10. The SFRC deep beam with 10 mm CA compared to that of CA20-10. Moreover, mutually SFRC deep beams with CA10 and CA20-10 concrete exhibited complete asymmetric displacement response to incremental loading. Naturally, the non-uniform fiber dispersion and aggregate interlock produced the different shear resistance on both sides of the beam. The failure pattern of SFRC deep beam with CA10 and CA20-10 concrete have similar failure (shear) mode. The major cracks developed between in the constant shear region were the cause of the brittle beam failure.

Keywords: Beams; Fiber reinforced concrete; Shear failure; Steel fiber reinforced concrete (SFRC); Aggregate.

INTRODUCTION

The use of reinforced concrete (RC) deep beams is architecturally preferable as it facilitates enormous open space. Also, various structural elements can be classified as “deep beams”, such as laterally loaded slabs, shear walls and pile caps (Sachan and Kameswara Rao, 1990). However, the understanding of the entire structural behavior of deep beam constitutes a challenging engineering problem, since various modes of failures have been observed for such beams (Roberts and Ho, 1982). The critical concern of RC deep beam designers is the catastrophic failure caused by the shear cracks those propagates rapidly in the web due to high inclined tensile stresses arise from the shearing loads. Various Research evidence has shown that the introduction of steel fiber to concrete to produce steel

fiber reinforced concrete (SFRC) improves the structural performance of deep beams (Al-Ta'an and Al-Feel, 1990). Adebar et al. (1997) have investigated the shear and ductility of rectangular SFRC beams under three-point loading. These investigators reported that by inclusion 0.4% and 0.6% hooked steel fibers having an aspect ratio of 60; the shear strength improves by 67% and 90% respectively. A research study on I-beams without stirrups conducted by Tan et al.(1993) yields that the use of hooked steel fibers can improve the shear strength of up to 73%. Ashour et al. (1992) investigated the shear behavior of SFRC beams with no stirrups fabricated from high strength concrete. They demonstrated that the incorporation of steel fibers alter the brittle behavior of these beams in a ductile manner, especially for beams having a higher a/d ratio. In

addition, they showed that the use of steel fiber increases the stiffness of the beam, which decreases the deflection of the beams.

The properties of SFRC significantly depends on fiber content, fiber distribution and the bond between the fiber and concrete (Dinh, 2009). The effect of using steel fibers in the concrete is typically studied by varying fiber volume fraction and the type of fiber, which includes changing the fiber aspect ratio, fiber length, and fiber strength (Mansur et al., 1986, Swamy et al., 1993, Shin et al., 1994, Kwak et al., 2002).

Reinforced concrete beams with or without web reinforcement, which subjected to combined flexural and shearing stress, can fail without ample warning in shear (Dinh, 2009, Roberts and Ho, 1982). Traditionally, reinforced concrete beams are reinforced with stirrups to avoid failure due to tensile shearing stresses. The inclusion of short and discrete metallic fibers with an aspect ratio L/d of about 20 to 100 in concrete has been proved to enhance the shear strength by resisting formation and growth of cracks (Bentur and Mindess, 2006). A steel fiber forms bridge to transfer tensile stresses across the crack, and thus mitigates its propagation. The same function of steel fibers is made by aggregates, which known as “aggregate interlock”. However, it is known that the coarse aggregates have a significant influence on the shear behavior of deep beams; its contribution to the shear strength of this beam is an open question.

Since concrete starts to fracture at very low tensile stresses, it is known as “brittle” material. However, their geometrical proportions make these beams viable to total shear failure without ample warning. The coarse aggregates form a bridge to transfer tensile stresses across the crack,

and thus mitigates its propagation, which known as “aggregate interlock”. However, it is known that the coarse aggregates have a significant influence on the shear behavior of deep beams; their contribution to the shear strength of this beam is not understood yet. It should be noted that it is believed that SFRC beams fabricated from concrete with greater aggregate sizes will have higher shears strength due to the increase in the aggregate bridging. To minimize the effects of aggregate on the shear behavior of SFRC, most of the researchers used the maximum aggregate size of 10 mm. Up to now, the effect of aggregate size on the shear behavior of SFRC beams has not been appropriately investigated. Scarce information on the literature is available on the contribution of aggregate on the shear strength of RC structural elements. Sherwood et al. (2007) have conducted an experimental study on the shear behavior of full-scale thick RC slabs. The reported that the aggregate interlock plays an essential role in the shear strength of these slabs with a significant influence of the maximum aggregate size. Also, they reported that the ACI method of prediction the shear strength is not conservative for such slabs. The primary objective of this study is to investigate the impact of coarse aggregate size on the fracture mechanics of SFRC deep beams.

Materials and Methods

Materials

In this experimental study, conventional concrete was developed as utilized to prepare the beam specimens. Ordinary Portland cement (PC) with an average grain size of 13 μm and complying the specifications of ASTM C150 was used as the cementitious material to establish the normal concrete. Table 1 presents the physical and chemical properties of the used PC. Following ASTM C33 requirements, 65% fine and 35% crushed aggregate (by weight) with entire fineness

modulus of 2.58 were mixed in this normal concrete. Two different sizes (10 mm and 20 mm) of the coarse aggregate (CA) were used in this investigation. The first mixture of SFRC incorporated both sizes of CA. However, the second one was prepared with only 10 mm CA. The physical properties of aggregate employed

to develop the concrete and related mix designs are presented in Table 2 and Table 3, respectively. In Table 3, the first mixture of SFRC was designated as MCA to indicate the mixed (10 mm and 20 mm) CA, whereas the second mixture was labeled as 10CA as it incorporated only 10 mm CA.

Table 1. Physical and Chemical Properties of PC

| Oxide (%) | | | | | | | | Relative density | Fineness (m ² /kg) |
|------------------|--------------------------------|--------------------------------|-------|------|-------------------|-----------------|------|------------------|-------------------------------|
| SiO ₂ | Al ₂ O ₃ | Fe ₂ O ₃ | CaO | MgO | Na ₂ O | SO ₃ | LOI | | |
| 20.2 | 5.49 | 4.12 | 65.43 | 0.71 | 0.26 | 2.61 | 1.38 | 3.14 | 373 |

Table 2. Properties of aggregates in the developed concrete

| Material | Unit Weight (kg/m ³) | Specific gravity | Absorption (%) |
|-------------------|----------------------------------|------------------|----------------|
| Sand (fine) | 1725 | 2.63 | 0.77 |
| Sand (coarse) | 1552 | 2.68 | 1.52 |
| Aggregate (10 mm) | 1570 | 2.65 | 1.45 |
| Aggregate (20 mm) | | | |

Table 3. Mix design of concrete (in kg/m³)

| Mix. | CA size (mm) | CA | PC | Steel fibers | Water | FA | | Superplasticizer (Glenium 51) |
|---------|--------------|------|-----|--------------|-------|------|---------|-------------------------------|
| | | | | | | fine | Crushed | |
| CA10-20 | 10 | 310 | 370 | 157 | 173 | 287 | 533 | 1.85 |
| | 20 | 724 | | | | | | |
| CA10 | 10 | 1034 | | | | | | |

Fig. 1 displays the grain size distribution of PC and the fine and coarse aggregates used in the concrete. The properties of steel fibers (as per ASTM A820 requirements) used in the preparation of SFRC are given in Table 4. It worth noting that to ensure the uniform dispersion of steel fibers in concrete, an improved polycarboxylic ether-based polymer superplasticizer (commercially known as Glenium 51), with a relative density of 1.1 and a dry extract of 36%, was utilized (Table 3). Additionally, the steel rebar exploited for beam reinforcement had yielding strength of 550 MPa.

Methods

Mixing method

In this investigation, two SFRC deep beams with 10mm and 20 mm aggregate nominal size were developed by using a

conventional concrete mixture (Table 3). This concrete was prepared by mixing the PC, fine and coarse aggregates in their dry state up to a satisfactory consistency. At that moment, this consistent mixture was supplied with absorption water for one minute. Later, mixing water and the dose of super plasticizer were added, and the wet mixture was blended - stopped consecutively for three minutes by using Hobart mixer (30-liter capacity) at the moderate pace of rotation (about 180 rpm). Subsequently, steel fibers were gradually added with a small quantity to achieve an optimal distribution within the mixture at a slow rotation rate of the mixture (about 50 rpm) for three minutes. Next, to fiber addition, the speed of the mixer was changed to moderate rate up to a standardized mixture of SHCC was accomplished. Eventually, the resulted SFRC was cast into the formwork of beam

in 50 mm layers. Cylindrical test specimens for evaluating the compressive

strength as per ASTM C 39 recommendations were established.

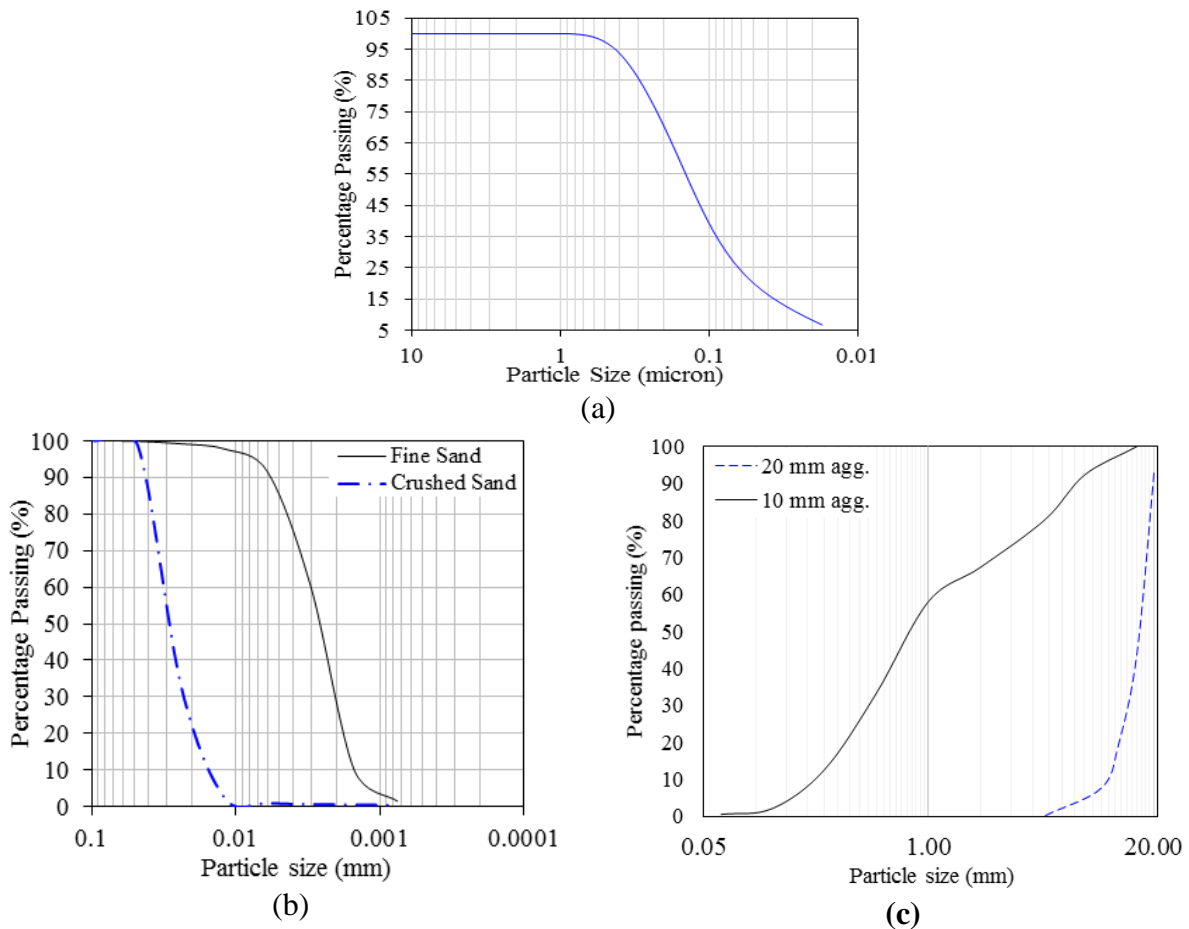


Fig. 1. Particle size distribution: a) PC, b) fine aggregate, and C) coarse aggregate

Table 4. Properties of steel fibers

| Type | Length (mm) | Diameter (mm) | Tensile Strength (MPa) | Young's Modulus (GPa) | Elongation (%) |
|------------|-------------|---------------|------------------------|-----------------------|----------------|
| DRAMIX® 3D | 35 | 0.55 | 1.35 | 210 | ±7.5 |

Casting and Curing of Beam specimens

Fig. 2 and displays the schematic diagram of the SFRC deep beam specimens, respectively. The dimensions of the beam specimens were 200 mm × 600 mm × 2500 mm. Five steel rebars of size 20 mm were positioned at the bottom, and two of the same diameter was located at the top of the beam specimens. The tensile reinforcement is selected to be about 1% of the concrete area to minimize the dowel contribution to the shear strength of beams. Additionally, the standard 90° hook was used to the top reinforcement, and the

bottom reinforcement was welded to 150×150×12 mm³ steel plate to ensure a proper bond of steel and concrete. This steel plate was required to avoid the lack of dispersion problem of SFRC at the high volume of steel fibers (2%) in the condition that a standard 180° hook was employed for the bottom reinforcement. It worth noting that only three closed 8-mm stirrups were used on each side of the beams to avoid the load shear failure at those parts. Moreover, for the tested beams, the span to depth ratio was maintained as 0.5 to force the beam to

have the real shear behavior under the displacement controlled loading conditions.

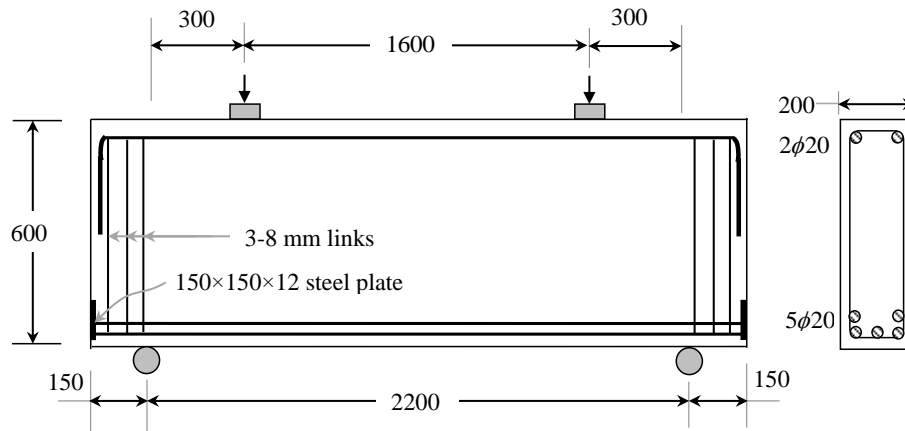


Fig 2. The schematic diagrams of the SFRC deep beam specimens

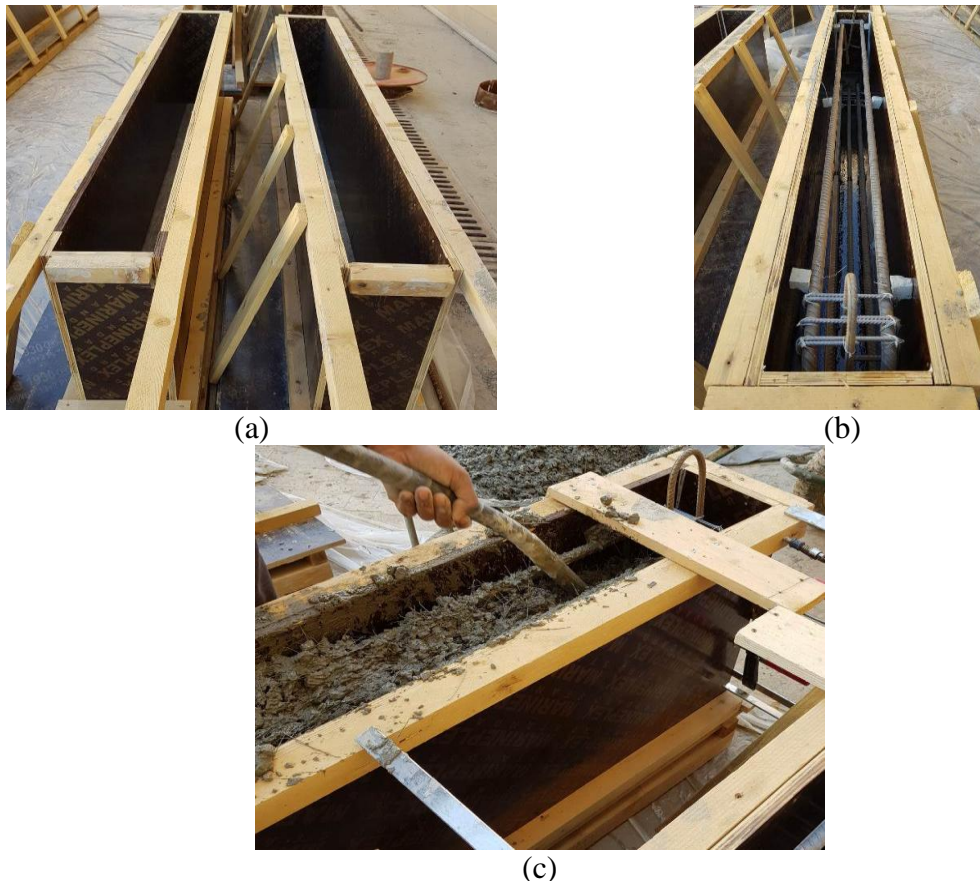


Fig. 3. The establishment method of the SFRC deep beam specimens:

- a) forms, b) placing steel cage, and c) pouring and compaction of the SFRC

Testing methods

TONITEK[®] compression testing machine (3000 kN capacity, Fig. 4) was utilized for evaluating the compressive strength of the normal concrete under loading rate of

0.006 mm/s. The specimens for the compressive strength test were of size 150 mm diameter ×300 mm length by ASTM C 31. Additionally, the properties of steel rebars were acquired using INSTRON[®]

(600 kN capacity) with loading speed of 0.2 mm/s. Moreover, AMSELOR[®] (Fig. 5) with four columns hydraulic testing machine (2000 kN capacity) was used to conduct the four-point test of SFRC deep beams. Fig. 6 shows the instruments used to acquire results of the flexural behavior of SFRC deep beams. To evaluate the deflection of beams, three TOKYO SOKKI[®] LVDT's were positioned below the beam (two at 300 mm of each support and one at the center of the beam). Furthermore, to investigate the strain response of steel and concrete, three strain gauges (Fig. 6) were attached at the middle

of the beam (one at the top of concrete and two on the tensile steel rebars). Additionally, four strain gauges (two on each side) were attached to the face of the beam where shear failure (strut location) is anticipated to exist. It worth noting that the incremental displacement loading on this machine was performed at 0.033 mm/s rate. As well, all the instrumentation were connected to TDS-630- TOKYO SOKKI[®] data acquisition system. At the end of the test, high-quality photos were taken to evaluate the failure pattern of SFRC deep beams.



Fig. 4. TONITEK[®] compression testing machine



Fig. 5. Testing machines: the beam specimens using the AMSELOR[®] hydraulic testing machine

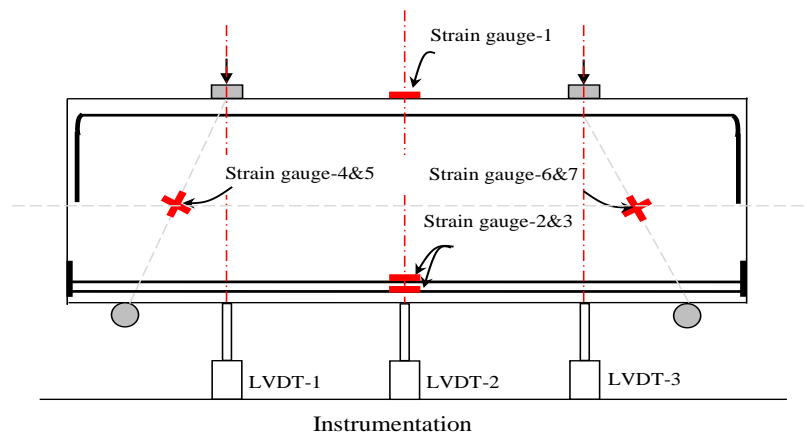


Fig. 6. The Instrumentations of the SFRC deep beam specimens

Flexural performance and failure patterns of SFRC deep beams with various sizes of aggregate

Fig. 7 shows the load-deflection curves for the SFRC deep beams at centerlines and load lines of beams. Fig 7a demonstrates that the size of aggregate has very little influence (only 1.3% difference of ultimate deflections) on the ductility of beams (as both SFRC deep beams with CA10 and CA20-10 concrete failed at 28.3 mm and 27.9 mm, respectively). However, SFRC deep beam with 10 mm CA exhibited higher load capacity concerning that of mixed 20mm and 10mm CA (the ultimate load of DB-2.0-1 increased by about 71% concerning DB-2.0-2). This result perhaps attributed to the better fiber dispersion in the beam with 10mm aggregates about that with diversified aggregates (20mm and 10mm). This finding agrees with that reported by Tasdemir et al. (Tasdemir et al., 1996). These researchers revealed that the cement-aggregate border had an abundance of CH and low-density CSH. Therefore, the cracks frequently established on this fragile interface. In

their study, it was concluded that the fracture toughness reduced notably for large diameter of aggregate which increases the brittleness of concrete. Unlike the findings reported by Ghasmi et al. (2018) on the influence of aggregate size on the fracture behavior of self-consolidated SFRC (SCSFRC) beams. These investigators reported that the maximum size of aggregate for SCSFRC is 12.5 mm as the ductility of slender beams dramatically decreases with 19 mm aggregate size.

Fig. 7b reveals that both SFRC deep beams with CA10 and CA20-10 concrete underwent asymmetric deformation as their displacement response to incremental loading at the left and the right load lines were uneven. However, at low loading (up to about 250 kN, which seems to be corresponding to the initiation of the first shear crack), the deflection of the load's lines was almost typical. As expected, the non-uniform fiber dispersion and aggregate interlock produced the different shear resistance on both sides of the beam.

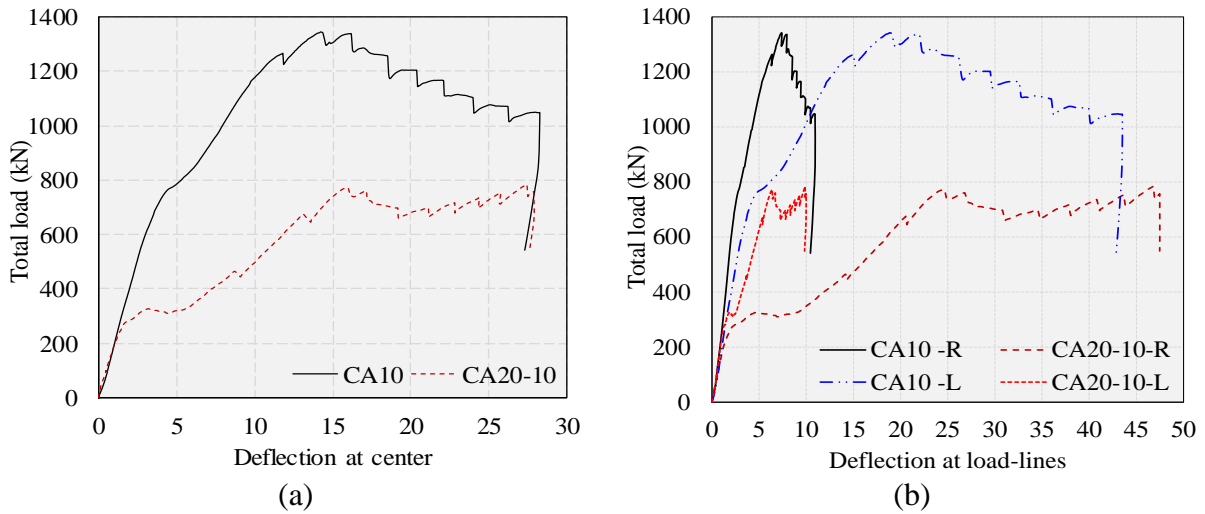


Fig. 7. Load-deflection curves of SFRC deep beams
a) center, and b) load lines (left-L and right-R)

Fig. 8 displays the strain curves for the SFRC deep beams at the top of concrete and the two levels of steel rebars. About concrete, Fig. 8a evidences that the SFRC deep beams with mixed aggregate (CA20-10) exhibited higher compressive strains concerning that with 10 mm aggregate for strains low than that corresponding to the ultimate strength of concrete (0.002). After that, the strains of SFRC deep beams with CA10 became more with respect to that of CA20-10. This finding demonstrated that the impact of the aggregate interlock of aggregate with large size becomes inferior to that of aggregate sizes when the extreme compressive

stresses exceeds the ultimate strength of concrete. Moreover, Fig. 8a indicates that the ductility of SFRC deep beams with CA10 was slightly higher than that with CA20-10 (about 11.4% strain difference), which may be attributed to the improved fiber-matrix interactions for small aggregate sizes. As regard to steel rebars, Fig. 8b reveals that the steel strains of SFRC deep beams with CA10 were mostly higher than that of CA20-10, which confirmed that the ductility of CA10 beam was superior. However, this phenomenon was altered for steel strains below 0.002 (similar behavior was observed for concrete strains).

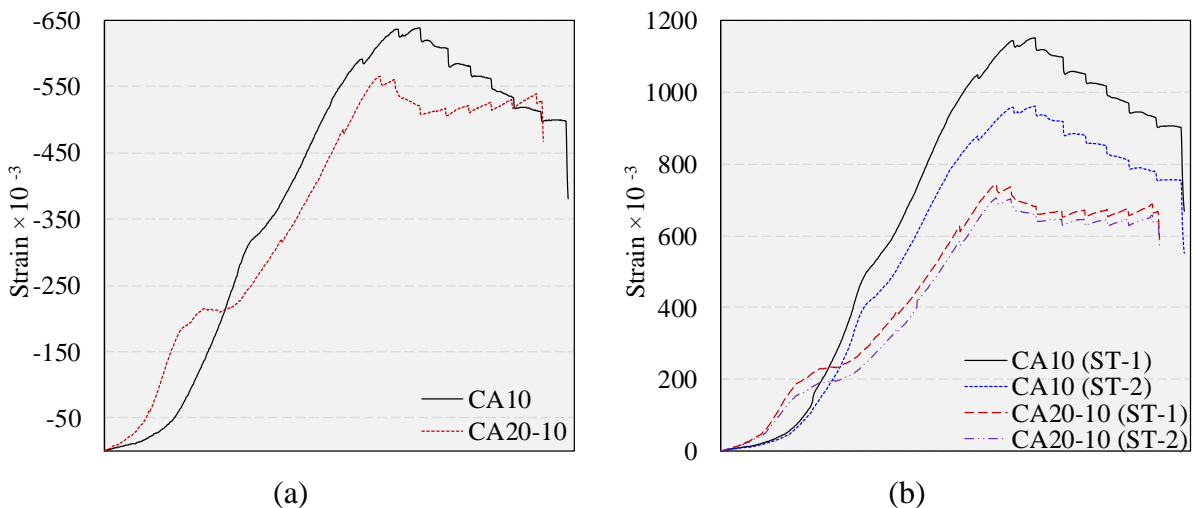


Fig. 8. Strain of a) concrete, and b) steel

The strain curves of SFRC deep beams at strut and tie regions of concrete at the left and right support-load lines are presented in Fig. 9. This figure indicated that the strut-tie strains of SFRC deep beams of 10 mm aggregate size are more significant than that with 20-10 mm. This finding

demonstrated the higher load capacity of CA10 beams with respect to that of CA10-20. Additionally, this figure suggested that axisymmetric deformations of beams existed up to ascertain limit, after which cracking prorogated on the weaker side of the beam.

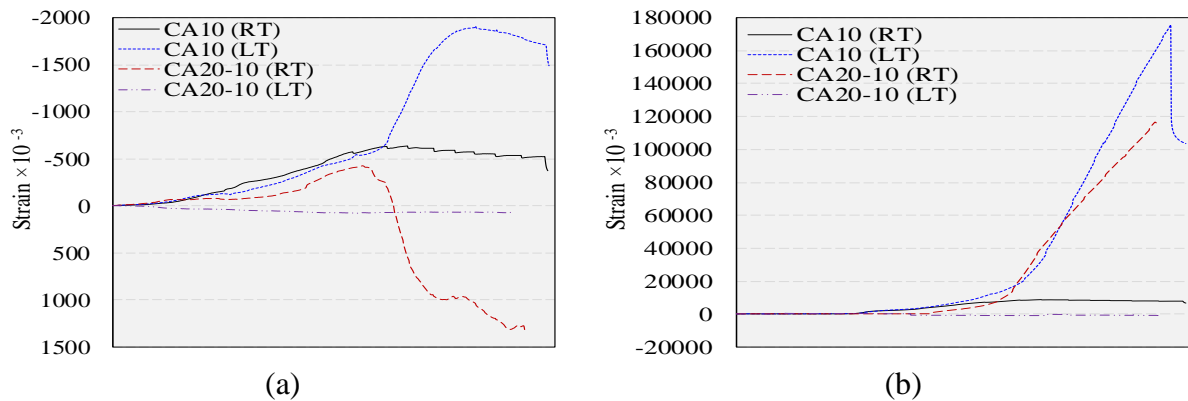


Fig. 9. Strain of concrete in the strut-tie region: a) strut, and b) tie

Failure pattern of SFRC deep beams with various sizes of aggregate

Fig. 10 presents the failure (cracking) pattern of SFRC deep beam with CA10 and CA20-10 concrete. This figure demonstrated that both beams have similar failure (shear) mode. It worth noting the numbers shown beside the cracks constitutes the total load on the beam at which the cracks was visually detected. Moreover, flexural cracks began between the loading lines (constant moment region), then, the major shear cracks developed between the support-loading lines (constant shear region). These main shear cracks were the cause of brittle beam failure. The total load corresponding to the initiation of the primary shear crack in SFRC deep beam with CA10 (750 kN) was notably less than that with CA20-10 concrete (1100 kN). Another observation for SFRC deep beam with CA20-10 was that it failed by bearing failure (support), which may be attributed to the honeycombs caused by the larger sizes aggregates and fiber dosage.

CONCLUSIONS

This experimental study was designed to investigate the effects of coarse aggregate size on the response of SFRC deep beams to incremental displacement-controlled loading. The ductility of SFRC deep beams with CA10 was marginally higher than that of CA20-10, which was attributed to the improved fiber-matrix interactions for small aggregate sizes. The SFRC deep beam with 10 mm CA had notably higher load capacity with regard to that of CA20-10. This result was attributed to the improved fiber distribution in the beam with 10mm aggregates compared to that with mixed aggregates (20mm and 10mm). Both SFRC deep beams with CA10 and CA20-10 concrete exhibited complete asymmetric displacement response to incremental loading. Conversely, axisymmetric displacement response was observed for these beams at low loading conditions. Unsurprisingly, the non-uniform fiber dispersion and aggregate interlock produced the different shear resistance on both sides of the beam. In the state that the maximum compressive

stains were less than 0.002 (corresponding to the ultimate strength of concrete), the SFRC deep beams with CA20-10 showed the more magnificent top of concrete strains with respect to that with CA10. Next, to that strain, the SFRC deep beams with CA10 became more concerning that of CA20-10. This finding demonstrated the minor impact of aggregate interlock with large size compared to that of small dimensions. The failure pattern of SFRC deep beam with CA10 and CA20-10

concrete have similar failure (shear) mode. The flexural cracks initiated in the constant moment region, then, the primary shear cracks developed between in the constant shear region. These main shear cracks were the cause of brittle beam failure. The probability of honey-combs existence within the SFRC beam that caused by the larger size aggregates and fiber dosage may alter the pattern of failure to bearing instead of shear.

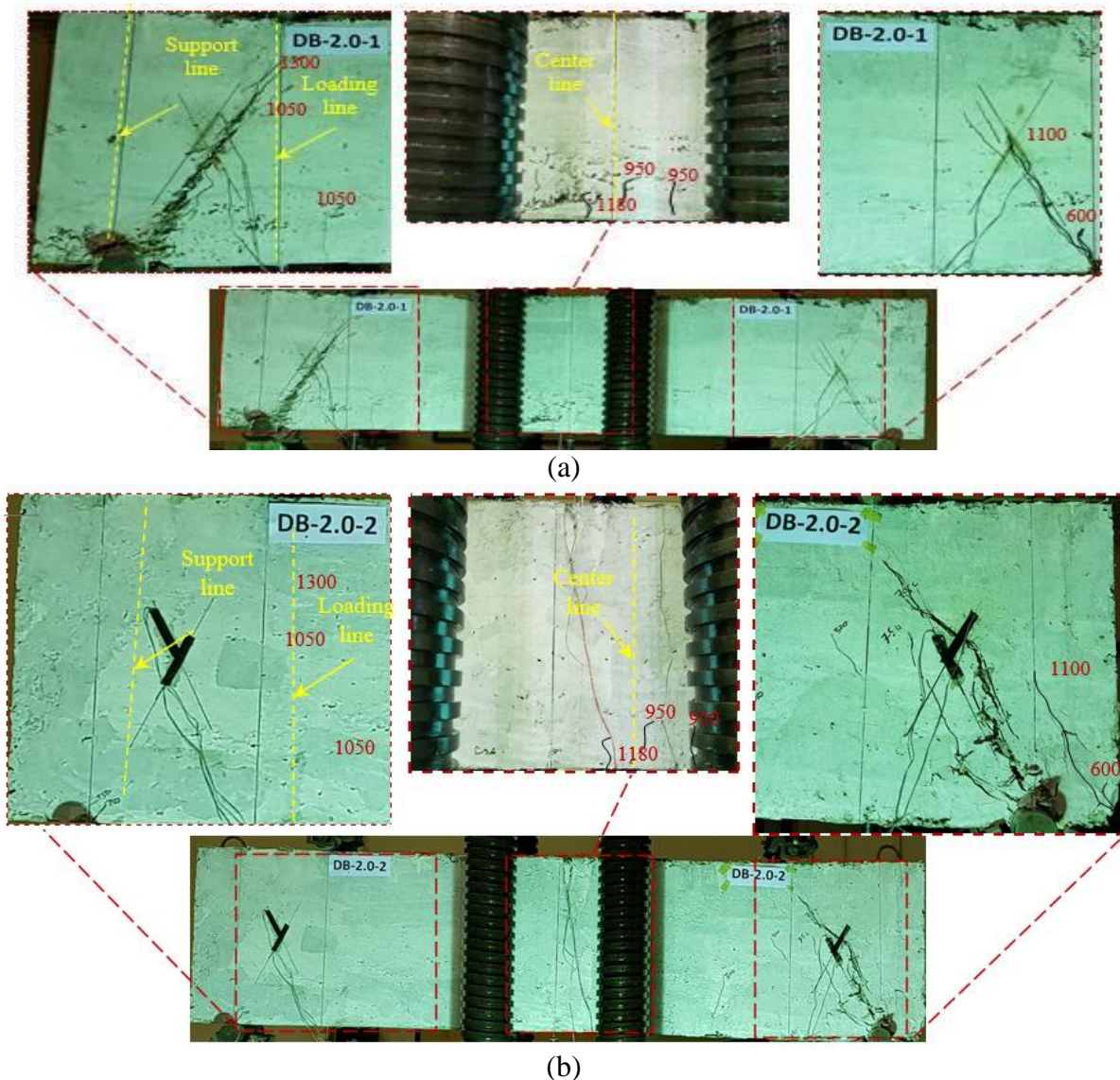


Fig. 10. Failure pattern of SFRC deep beam with:
a) 10 mm , and b) 20-10 mm size of aggregate

ACKNOWLEDGEMENT

The author would like to extend his appreciation to the Research Center, College of Engineering Center at King Saud University for funding this work through the project No. 438/6.

REFERENCES

1. Adebar, P., Mindess, S., Pierre, D. S.-. & Olund, B. 1997. Shear tests of fiber concrete beams without stirrups. *ACI Structural Journal*, 94.
2. Al-Ta'an, S. & Al-Feel, J. 1990. Evaluation of shear strength of fibre-reinforced concrete beams. *Cement and Concrete Composites*, 12, 87-94.
3. Ashour, S. A., Hasanain, G. S. & Wafa, F. F. 1992. Shear behavior of high-strength fiber reinforced concrete beams. *ACI Structural Journal*, 89.
4. Bentur, A. & Mindess, S. 2006. *Fibre reinforced cementitious composites*, Taylor & Francis, New York.
5. Dinh, H. H. 2009. *Shear behavior of steel fiber reinforced concrete beams without stirrup reinforcement*. University of Toronto.
6. Ghasemi, M., Ghasemi, M. R. & Mousavi, S. R. 2018. Investigating the effects of maximum aggregate size on self-compacting steel fiber reinforced concrete fracture parameters. *Construction and Building Materials*, 162, 674-682.
7. Kwak, Y.-K., Eberhard, M. O., Kim, W.-S. & Kim, J. 2002. Shear strength of steel fiber-reinforced concrete beams without stirrups. *ACI Structural Journal*, 99.
8. Mansur, M., Ong, K. & Paramasivam, P. 1986. Shear strength of fibrous concrete beams without stirrups. *Journal of Structural Engineering*, 112, 2066-2079.
9. Roberts, T. & Ho, N. 1982. Shear failure of deep fibre reinforced concrete beams. *International Journal of Cement Composites and Lightweight Concrete*, 4, 145-152.
10. Sachan, A. & Kameswara Rao, C. 1990. Behaviour of fibre reinforced concrete deep beams. *Cement and concrete composites*, 12, 211-218.
11. Sherwood, E. G., Bentz, E. C. & Collins, M. P. 2007. Effect of aggregate size on beam-shear strength of thick slabs. *ACI Structural Journal*, 104.
12. Shin, S.-W., Oh, J.-G. & Ghosh, S. 1994. Shear behavior of laboratory-sized high-strength concrete beams reinforced with bars and steel fibers. *ACI Special Publication*, 142.
13. Swamy, R. N., Jones, R. & Chiam, A. T. 1993. Influence of steel fibers on the shear resistance of lightweight concrete I-beams. *ACI Structural Journal*, 90.
14. Tan, K., Murugappan, K. & Paramasivam, P. 1993. Shear behavior of steel fiber reinforced concrete beams. *ACI Structural Journal*, 90.
15. Tasdemir, C., Tasdemir, M. A., Lydon, F. D. & Barr, B. I. 1996. Effects of silica fume and aggregate size on the brittleness of concrete. *Cement and Concrete Research*, 26, 63-68.